J. Quant. Spectrosc. Radiat. Transfer Vol. 46, No. 5, pp. 463–471, 1991
Printed in Great Britain

0022-4073/91 $3.00 + 0.00
Pergamon Press plc

RAPID COMPUTATION OF THE RADIATIVE ABSORPTION RATE IN THE ν_3 MODE OF MESOSPHERIC AND LOWER THERMOSPHERIC OZONE

MARTIN G. MLYNCZAK†
Theoretical Studies Branch, Atmospheric Sciences Division, NASA Langley Research Center, Mail Stop 401B, Hampton, VA 23665-522

S. ROLAND DRAYSON
Department of Atmospheric, Oceanic, and Space Sciences, University of Michigan, 2455 Hayward, Ann Arbor, MI 48109, U.S.A.

(Received 29 January 1991)

Abstract—We have developed an algorithm to calculate rapidly and accurately the rate (photons-molecule^{-1}-sec^{-1}) at which the ozone ν_3 fundamental band absorbs i.r. radiation in the terrestrial upper mesosphere and lower thermosphere. Accurate knowledge of this rate is essential for studies of non-LTE processes in ozone and for estimating ozone concentrations from measurements of non-LTE i.r. emission from the middle atmosphere. In our algorithm, the 1252 ozone ν_3 fundamental lines that govern radiative absorption are divided into 13 groups according to line strength. The absorption rate due to a single line representative of the mean line strength of each group is then calculated. The total absorption rate is obtained by multiplying the absorption rate for each mean line by the total number of lines within each group and adding the resultant products for all 13 groups. We also incorporate several other approximations, such as assuming that each mean line has the same Voigt line shape, which significantly reduces the number of Voigt function evaluations. The algorithm preserves the accuracy of detailed, time-consuming line-by-line approaches while requiring only a fraction of the CPU time of such techniques.

1. INTRODUCTION

One of the most important excitation mechanisms of the ν_3 fundamental band of ozone in the upper mesosphere and lower thermosphere is the absorption of radiation emitted by lower mesospheric and upper stratospheric ozone.[1–3] Radiative absorption drives this transition from local thermodynamic equilibrium (LTE) and is the dominant loss mechanism of ground state ozone in the nighttime upper mesosphere and lower thermosphere.[1] Emission from the ν_3 fundamental band of ozone (centered at 1042.1 cm^{-1}) is also frequently observed in remote sensing experiments. It is therefore necessary to have an accurate knowledge of the radiative absorption rate in order to correctly calculate the ν_3 fundamental source function for use in non-LTE studies[4] and for use in algorithms designed to determine the ozone concentration from i.r. emission measurements.

The expression for the radiative absorption rate in photons-molecule^{-1}-sec^{-1} at an altitude z can be readily derived. The amount of energy per unit time per unit solid angle per unit frequency, dE_ν, absorbed from an individual pencil of radiation is given by (e.g., Chandrasekhar[5])

$$dE_\nu = k_\nu I_\nu, \tag{1}$$

where k_ν is the absorption cross section (cm^2) and I_ν the specific intensity. The total absorbed energy per unit time is obtained by integrating Eq. (1) over solid angle and frequency,

$$E = \int_\Omega \int_\nu dE_\nu = \int_0^{4\pi} \int_{-\infty}^{\infty} k_\nu I_\nu \, d\Omega \, d\nu, \tag{2}$$

†To whom all correspondence should be addressed.

where $d\Omega$ indicates integration over solid angle and $d\nu$ integration over frequency. The radiative absorption rate $\mathscr{R}$ in units of photons-molecule^{-1}-sec^{-1} is obtained by dividing dE_ν by $h\nu$, the photon energy, prior to integrating over solid angle and frequency. Thus,

$$\mathscr{R} = \int_0^{4\pi} \int_{-\infty}^{\infty} (k_\nu / h\nu) I_\nu \, d\Omega \, d\nu. \tag{3}$$

$\mathscr{R}$ is the quantity frequently used in statistical equilibrium models of ozone.[1-4]

Formal evaluation of Eq. (3) for ozone is extremely time consuming because of the number of atmospheric layers involved, the number of spectral lines, and the required spectral resolution. Different researchers have employed various approximations in order to evaluate the integral in Eq. (3) readily. Rawlins[3] used a spectrally-averaged intensity to evaluate $\mathscr{R}$, i.e.,

$$\mathscr{R} = S_b \bar{I}_\nu / h\nu_0, \tag{4}$$

where S_b is the band strength, and ν_0 the frequency at band center. Solomon et al[2] solved the two-level problem for ozone using a Curtis-matrix formulation and they then inferred $\mathscr{R}$. However, neither of these approaches is preferable to the direct evaluation of $\mathscr{R}$. The Curtis-matrix approach used by Solomon et al is numerically unstable[2] and the Rawlins[3] approach will yield correct values only when the spectrally-averaged intensity $\bar{I}_\nu$ is equal to the intensity absorbed by each spectral line, which rarely occurs. Furthermore, Mlynczak[6] has shown that high-resolution, line-by-line accuracy is necessary in order to replicate correctly the correlation between the incident radiation and the absorption coefficient in the calculation of the absorption rate. Average intensities, even over narrow spectral intervals, cannot accurately simulate the integral of Eq. (3).

Through a series of approximations to and exploitations of the physics of radiative absorption by mesospheric and lower thermospheric ozone, we have developed a computationally fast algorithm to evaluate Eq. (3). The technique maintains the accuracy ultimately needed for correct source function evaluation, while significantly reducing the computation time from that required for direct calculations. The calculation of $\mathscr{R}$ between ~ 50 and ~ 110 km in steps of approx. 2 km (i.e., at 33 pressure levels) now requires about 1.6 CPU sec on a Digital Equipment Corp. VAX 11-785.

We describe the algorithm in Sec. 2. Radiative absorption rates calculated using detailed approaches are then compared with rates using our new approach described herein. We also compare the ozone ν_3 fundamental source functions calculated using the radiative absorption rates from both approaches.

2. APPROXIMATIONS IN THE EVALUATION OF $\mathscr{R}$

The first step in reducing the number of mathematical operations needed to compute $\mathscr{R}$ is to neglect the weakest lines of ozone that do not significantly contribute to the radiative absorption rate. Of the 6992 ν_3 fundamental ozone lines listed on the 1986 HITRAN database (Rothman et al[7]), the 1252 lines with strengths (at 296 K) greater than 10^{-21} cm^{-1}-molecule^{-1}-cm^2 constitute 97.3% of the band strength. We only consider these 1252 lines since it was shown by Mlynczak[6] that the neglected weak lines contribute negligibly to $\mathscr{R}$. Next, we divide the 1252 lines into groups of lines according to line strength. Within each group, we calculate the mean line strength and the mean air-broadened Lorentz halfwidth. Linear weighting is used because of the small range of line strength employed in defining the groups. Each group is then assigned a mean frequency centered about 1040 cm^{-1}. Partitioning the lines in this way results in 13 groups which are detailed in Table 1. The next step is to define a strength-weighted, air-broadened Lorentz halfwidth for the entire set of lines, using mean parameters from the groups of lines, viz.

$$\alpha_L^S = \sum_{i=1}^{13} S_i N_i \alpha_L^i \Big/ \sum_{i=1}^{13} S_i N_i. \tag{5}$$

Here, S_i is the mean line strength in group i, N_i the number of lines in group i, and α_L^i the mean air-broadened halfwidth in group i. A strength-weighted frequency ω^S is also calculated by substituting the frequencies found in Table 1 into Eq. (5) in place of the α_L^i.

Table 1. Mean spectral line parameters used in the rapid computation of the radiative absorption rate. Note that 4(−20) is read as 4×10^{-20}. The units of the mean Lorentz halfwidth are cm^{-1}.

S_{min}	S_{max}	Number of lines	S_{mean}	α_L(mean)	ν (cm^{-1})
4(-20)	5(-20)	3	4.050(-20)	0.0698	1034.5
3(-20)	4(-20)	91	3.458(-20)	0.0691	1035.5
2(-20)	3(-20)	136	2.469(-20)	0.0667	1036.5
1(-20)	2(-20)	246	1.439(-20)	0.0658	1037.5
9(-21)	1(-20)	29	9.449(-21)	0.0651	1038.5
8(-21)	9(-21)	44	8.426(-21)	0.0650	1039.5
7(-21)	8(-21)	42	7.515(-21)	0.0646	1040.5
6(-21)	7(-21)	51	6.487(-21)	0.0654	1041.5
5(-21)	6(-21)	68	5.529(-21)	0.0645	1042.5
4(-21)	5(-21)	70	4.531(-21)	0.0643	1043.5
3(-21)	4(-21)	104	3.449(-21)	0.0642	1044.5
2(-21)	3(-21)	115	2.484(-21)	0.0639	1045.5
1(-21)	2(-21)	253	1.430(-21)	0.0636	1046.5

The radiative absorption rate is then evaluated for each of the 13 mean lines. We assume the same Voigt line shape for each line and the Voigt parameters are calculated from α_L^S and from ω^S. The routine developed from Drayson[8] is used to evaluate the Voigt function. We obtain the total radiative absorption rate by multiplying the rate for an individual mean line by the total number of lines within that group and adding the resultant products for all 13 groups. The temperature dependence of the lines is handled by using the following empirical correction:

$$S(T) = S(T_0)(C_0 + C_1 T + C_2 T^2). \tag{6}$$

In this fashion the band strength is preserved and the constants C_0, C_1, and C_2 are determined by fitting the expression

$$S_b(T) = S_b(T_0)(C_0 + C_1 T + C_2 T^2), \tag{7}$$

using band strengths as functions of temperature derived from the formula

$$S_b(T) = \sum_j^{\text{all } \nu_3} S_j(T_0) \exp\left[-\frac{E''}{k}\left(\frac{1}{T} - \frac{1}{T_0}\right)\right] \frac{Q(T_0)}{Q(T)} \left(\frac{T_0}{T}\right)^{1.5}, \tag{8}$$

where E'' is the lower rotational state energy, T_0 is 296 K, and Q represents the vibrational partition function. The sum is evaluated using all 6992 ozone ν_3 fundamental lines listed on the 1986 HITRAN database. Although the constants C_0, C_1, and C_2 are in principle different for each of the 13 groups, we have obtained good results by using the same constants for all groups.

The approximations described above reduce the number of spectral lines by nearly two orders of magnitude, with a corresponding decrease in the required number of evaluations of the Voigt function. Further reductions in the required operations are obtained by evaluating $\mathscr{R}$ only near the line center. As pointed out by Mlynczak,[6] radiation between the spectral lines is of no consequence in determining the radiative absorption rate. Therefore, it is only necessary to evaluate $\mathscr{R}$ near the line center, since mesospheric and lower thermospheric ozone lines are almost purely Doppler-broadened and are therefore extremely narrow. Furthermore, it suffices to evaluate $\mathscr{R}$ on one side of line center, as symmetric line shapes are assumed. The actual value of $\mathscr{R}$ is then evaluated by multiplying the calculated value of $\mathscr{R}$ by two. The spectral resolution employed in these calculations is $1.6666 \times 10^{-4}\ cm^{-1}$ (6000 quadrature points per cm^{-1}). The calculated value of $\mathscr{R}$ is essentially insensitive to contributions beyond about 4 Doppler halfwidths. This fact implies that $\mathscr{R}$ must be evaluated at 20 points in the spectral space per spectral line.

The computation of $\mathscr{R}$ is even further simplified by assuming that the radiation absorbed in the mesosphere and lower thermosphere is solely upwelling radiation from the vicinity of the warm stratopause. This assumption is valid because the ozone concentration and the kinetic temperature

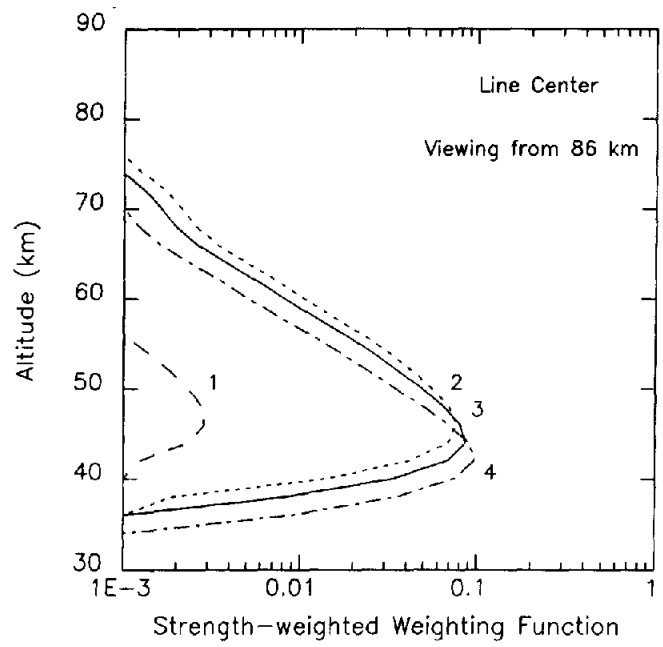

Fig. 1. The line strength-weighted weighting function $W_i(z)$ for evaluating the upwelling intensity at 86 km. The numerals 1, 2, 3, and 4 indicate the weighting function corresponding to the groups 1–4, respectively.

both decrease rapidly above the stratopause.[6] Furthermore, we simplify the integration over solid angle by assuming that the upwelling radiation is independent of the azimuthal angle (ϕ) and that the specific intensity integrated over zenith angle (Θ) is accurately approximated by the specific intensity at some mean zenith angle ($\bar{\Theta}$). These approximations can be expressed analytically as

$$\mathscr{R} = \int_{-\infty}^{\infty} \int_{0}^{2\pi} \int_{0}^{\pi/2} (k_\nu/h\nu) I_\nu(\Theta, \phi) \sin(\Theta)\, d\Theta\, d\phi\, d\nu, \tag{9}$$

which then simplifies to

$$\mathscr{R} = 2\pi \int_{-\infty}^{\infty} (k_\nu/h\nu) I_\nu(\bar{\Theta})\, d\nu. \tag{10}$$

We evaluate $I_\nu(\overline{\Theta})$ at a given altitude for $\sec(\overline{\Theta})$ equal to 1.667 using the expression

$$I_\nu(\bar{\Theta}, z) = \int_{0}^{z} B_\nu[T(z)] \frac{\Delta\tau}{\Delta z}\, dz, \tag{11}$$

where B_ν is the Planck blackbody function and $(\Delta\tau/\Delta z)$ is the weighting function corresponding to the path through a plane-parallel atmosphere at a zenith angle of $\bar{\Theta}$. The sensitivity of the calculation to the assumed value of $\bar{\Theta}$ will be discussed in Sec. 3.

Table 2. Latitudes, local times, and seasons for the five case studies for which the two approaches to calculating the radiation absorption rate are compared.

Case	Latitude	Local Time and Season
1	35 N	Noon, Northern Hemisphere Winter
2	35 N	Midnight, Northern Hemisphere Winter
3	3 N	Midnight, Northern Hemisphere Winter (effectively tropical annual)
4	82 N	Noon, Northern Hemisphere Winter (effectively polar night)
5	82 S	Noon, Southern Hemisphere Summer

The validity of the upwelling radiation assumption can be seen by examining Fig. 1, which shows the strength-weighted weighting function

$$W_i(z) = \Delta\tau(z) S_i N_i / \sum_{j=1}^{13} S_j N_j \tag{12}$$

for the first four mean lines, evaluated at the line center. The case presented is for evaluating the upwelling radiation at 86 km. The strength-weighted weighting function shows not only the altitudes which contribute to the upwelling radiation but also the relative importance of each of the first four groups of lines. The peak contribution to the radiation field at 86 km arises at 46, 46, 44 and 42 km, for groups 1–4, respectively. Groups 2, 3, and 4 contribute roughly the same to $\mathscr{R}$. It should be noted that these first four groups are responsible for nearly 75% of the total band strength and therefore approx. 75% of $\mathscr{R}$. The remaining groups of lines are weaker lines whose peak contributions will come from even lower in the atmosphere. Therefore, the approximation of using the upwelling radiation only is quite good. Mlynczak and Drayson[1] found it unnecessary to consider non-LTE source functions in the evaluation of $\mathscr{R}$ for ozone, which is further evidence that the downwelling component is negligible. The assumption of upwelling radiation is not valid in the lower mesosphere ($z < 60$ km). However, the ν_3 fundamental band is very nearly in LTE in this region, and it is therefore unnecessary to have highly accurate values of $\mathscr{R}$ below 60 km.

In our algorithm we explicitly calculate the upwelling intensity at every five pressure levels (approx. every 10 km) between 110 and 50 km. The upwelling intensity at intervening pressure levels is set equal to the value of the upwelling intensity calculated at the pressure level immediately below the intervening levels in altitude. $\mathscr{R}$ is then evaluated at each of the 33 pressure levels between 110 and 50 km using absorption coefficients evaluated for the conditions at each level. Finally, we assume that spectral line overlap is not significant because in the mesosphere and lower thermosphere the Doppler halfwidth is about 100 times smaller than the average line spacing of the 1252 strong ozone lines of the ν_3 fundamental. We will be comparing the results from our new approach with results from an approach that explicitly includes line overlap and that explicitly includes integration over solid angle. If line overlap is significant, then we do not expect the results from the two approaches to agree.

3. RESULTS

We compare the radiative absorption rates calculated from the approach described above with rates calculated by explicitly considering the contribution from the 1252 ozone ν_3 fundamental lines and by explicitly integrating the specific intensity over zenith angle. Absorption cross sections are calculated in this more detailed approach using the routines developed from Drayson.[8,9] The spectral resolution is 6000 quadrature points per cm^{-1} and the spectral interval over which $\mathscr{R}$ is evaluated is 986–1072 cm^{-1}. Integration over zenith angle is accomplished using 4-point Gaussian integration. We calculate only the upwelling component of the radiation field at each altitude between $\sim$50 and $\sim$110 km in steps of approx. 2 km. Calculations with this more detailed algorithm including downwelling (LTE) radiation changed the values of $\mathscr{R}$ by $< 0.01\%$ above 75 km. Finally, overlap of spectral lines is explicitly included in this detailed formulation.

We have calculated and compared radiative absorption rates for five case studies representing a variety of atmospheric conditions using both approaches described herein. The case studies are listed in Table 2. The kinetic temperature profiles and ozone concentration profiles at 35° N are from a one-dimensional photochemical model described in Sanders et al,[10] while the remaining profiles are from the two-dimensional model of Garcia and Solomon.[11] Listed in Table 3 is the percent difference in the radiative absorption rates as calculated by the two approaches for each of the five case studies. With the exception of Case 4, agreement between the calculated rates is generally better than 1.5% in the upper mesosphere and lower thermosphere ($z > 65$ km). Finally, the generally good agreement can also be taken as evidence that spectral line overlap is not a significant problem in the evaluation of $\mathscr{R}$.

The poorer agreement between the rates calculated for Case 4 is a consequence of the kinetic temperature structure of the atmosphere at 82° N. Figure 2 shows the temperature profiles for

Table 3. Percent difference (absolute values) in the radiative absorption rates calculated for Cases 1–5 using the two approaches described in the text. The altitudes are only approximate and can vary up to 4 km, depending on the season and latitude.

P(mb)	Z(km)	Case 1	Case 2	Case 3	Case 4	Case 5
0.101(-3)	104.0	0.024	0.952	0.783	3.645	0.774
0.134(-3)	102.0	0.342	0.659	0.541	3.825	0.253
0.179(-3)	100.0	0.580	0.530	0.410	3.773	0.088
0.239(-3)	98.4	0.724	0.396	0.263	3.688	0.368
0.318(-3)	96.8	0.930	0.313	0.198	3.550	0.671
0.424(-3)	95.2	1.003	0.212	0.093	3.377	0.930
0.566(-3)	93.6	1.110	0.137	0.052	3.106	1.190
0.754(-3)	92.0	1.138	0.093	0.023	2.787	1.398
0.101(-2)	90.5	1.166	0.056	0.087	2.611	1.552
0.134(-2)	88.9	1.166	0.056	0.144	2.395	1.672
0.179(-2)	87.4	1.155	0.100	0.063	2.090	1.736
0.238(-2)	85.9	1.155	0.031	0.121	2.092	1.791
0.318(-2)	84.3	1.161	0.025	0.144	2.010	1.794
0.424(-2)	82.8	1.089	0.044	0.133	1.752	1.771
0.565(-2)	81.2	0.993	0.031	0.070	1.444	1.714
0.753(-2)	79.6	0.822	0.300	0.221	0.947	1.570
0.100(-1)	77.9	0.655	0.326	0.327	0.424	1.472
0.134(-1)	76.2	0.581	0.321	0.363	0.150	1.336
0.179(-1)	74.5	0.512	0.239	0.399	0.802	1.199
0.238(-1)	72.8	0.431	0.050	0.399	1.480	0.989
0.317(-1)	71.1	0.113	0.585	0.493	1.974	0.671
0.423(-1)	69.3	0.077	0.044	0.258	2.671	0.435
0.564(-1)	67.5	0.042	0.595	0.123	3.484	0.160
0.753(-1)	65.7	0.187	1.319	0.621	4.388	0.137
0.100(-1)	63.9	0.309	2.015	1.101	5.405	0.380

Cases 3 and 4. The lapse rate in the 50–30 km layer in Case 4 is approx. 75% larger than in Case 3 and it is also much larger than at other latitudes. Therefore, even slight differences in the effective shapes and magnitudes of the weighting functions of each approach used to calculate $\mathscr{R}$ will translate into relatively large differences in $\mathscr{R}$ when such large lapse rates exist.

To verify that slight differences in the placement of the weighting functions in the presence of a large upper stratospheric lapse rate are responsible for the differences in the calculated values of $\mathscr{R}$ in Case 4, we evaluated the integral

$$N = \int_{z=0}^{z=110} B[T(z)]g(z - z')\,dz \tag{13}$$

for each of the five cases. Here, $B[T(z)]$ is the Planck function at altitude z, $g(z - z')$ is a Gaussian weighting function of full-width at half-maximum of 10 km, centered and peaking at z', and N represents the upwelling intensity. Varying z' by approx. 2 km (from the 1 to the 1.33 mbar surface) changed the value of N by 14% in Case 4. In contrast, N varied by only 4.2% in Cases 1 and 2, by only 3.0% in Case 3, and by only 0.85% in Case 5. We conclude that the accurate evaluation of $\mathscr{R}$ in the presence of large upper stratospheric lapse rates requires higher vertical resolution than the 2 km resolution which we have employed. Because of the good agreement obtained when using the two approaches to evaluate $\mathscr{R}$ in all other cases, we expect that high vertical resolution calculations using the new approach will yield accurate values of $\mathscr{R}$ for atmospheric conditions such as those in Case 4.

We anticipate that the small differences in the radiative absorption rates calculated using each of the two approaches will have negligible impact in the calculation of v_3 fundamental source functions. To verify this expectation we use the radiative absorption rates calculated by both

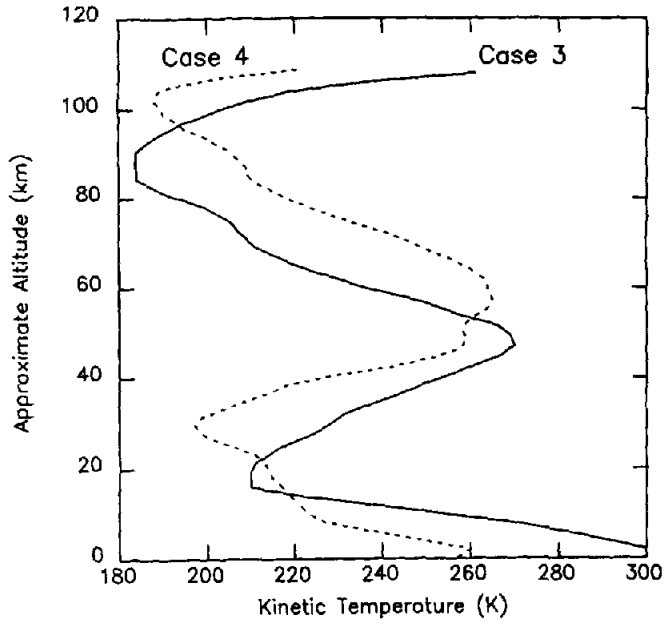

Fig. 2. Kinetic temperature profiles as a function of altitude for Cases 3 and 4. Note the strong lapse rate in the upper stratosphere in Case 4 relative to that in Case 3.

approaches in the statistical equilibrium model of Solomon et al[2], using the formulation and photochemistry described by Mlynczak and Drayson.[1] With the exception of Case 4, the calculated source functions are virtually insensitive to the differences in the values of $\mathscr{R}$ at the levels reported here. In Case 4, the source functions agree to better than 4%. It should be noted that under LTE conditions, an uncertainty in the kinetic temperature of only 2 K would yield an uncertainty in the ozone ν_3 fundamental source function of approx. 6%. We therefore conclude that the slight uncertainties in the calculated $\mathscr{R}$ values are of little consequence in the calculation of the source function and will therefore contribute very little to the uncertainty in ozone concentrations retrieved from i.r. emission measurements. Much larger uncertainties will exist due to lack of knowledge of the mechanisms and rate constants relevant to the chemical pumping and vibrational relaxation process.[1,12]

One of the assumptions employed in our new algorithm is that the specific intensity integrated over zenith angle could be approximated by the calculated specific intensity at one zenith angle. This approximation is possible in the upper mesosphere and lower thermosphere due to the fact that there is generally not a strong zenith angle dependence in the upwelling specific intensity from ozone. Our detailed calculations show a variation of approx. 3–10% in the specific intensity over the four Gaussian angles. Consequently, almost any mean zenith angle could be employed in the algorithm.

In order to investigate the range of $\mathscr{R}$ that could be expected under representative geophysical conditions, we calculate $\mathscr{R}$ from pole to pole at northern hemisphere winter solstice (at local noon) using our new approach. The temperature and ozone profiles are from the two-dimensional model of Garcia and Solomon.[11] The results are shown as a function of latitude and altitude in Fig. 3. The value of $\mathscr{R}$ varies by a factor of 2.6, and the variation is essentially due to the gradient from pole to pole in the temperature of the stratopause region. As is evident from Fig. 1, the radiative absorption rate in the upper mesosphere and lower thermosphere is governed by the kinetic temperature and ozone concentration in the vicinity of the stratopause. The increase in $\mathscr{R}$ evident around the high-latitude southern hemisphere mesopause (80–90 km) is due to the slightly larger band strength in the ν_3 fundamental band that occurs because of the very cold (150–165 K) summer mesopause temperatures.

Finally, we have calculated source functions for the ν_3 fundamental band using radiative absorption rates calculated with our new approach and the statistical equilibrium model (rates and mechanism) of Solomon et al.[2] The ratio of the source function to the local value of the Planck

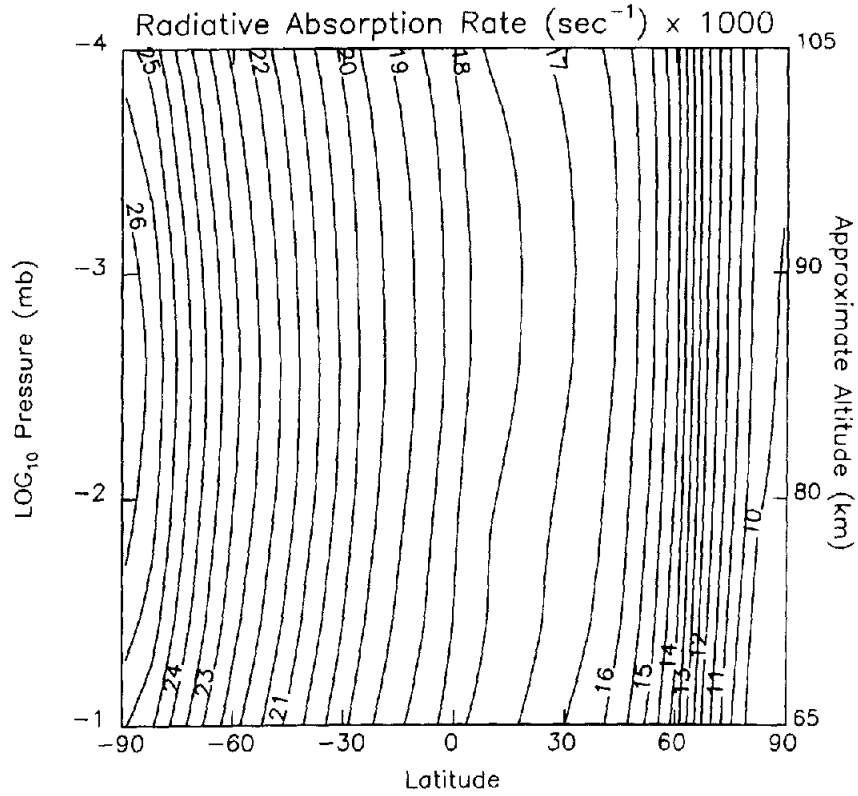

Fig. 3. Radiative absorption rate (photons-molecule^{-1}-sec^{-1} x 1000) as a function of latitude and altitude for the northern hemisphere winter at local noon.

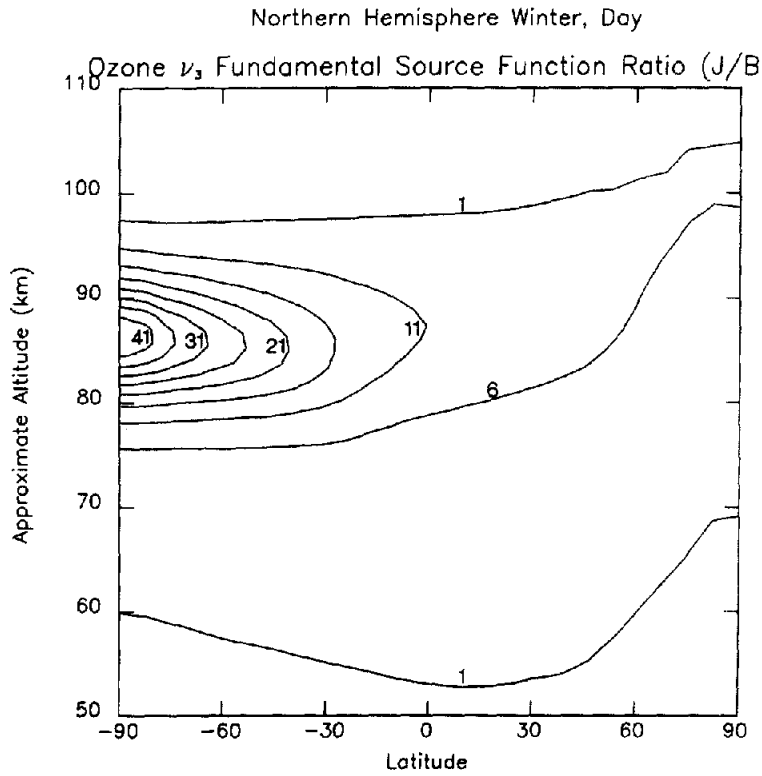

Fig. 4. Ratio of the ν_3 fundamental source function (J) to the local value of the Planck function (B) for northern hemisphere winter conditions. The contour interval is 5 units.

function is shown as a function of latitude and altitude in Fig. 4 for daytime conditions during northern hemisphere winter. The source function calculated from the Solomon et al[2] model is greater than the Planck function from about 55 to 105 km over a wide range of latitude. The strong enhancement near the summer pole is due to the cold kinetic temperatures of that region (150–170 K) coupled with the large values of the radiative absorption rate ($\mathscr{R}$) which are a result of the warm summer stratopause. The maximum enhancement of the source function over the Planck function is approximately a factor of 40 at the summer pole. Chemical pumping effects (due to the reaction of atomic oxygen with molecular oxygen) also serve to drive this transition from LTE, but such processes are of lesser importance in the determination of the enhancement of this source function. In contrast, the source function at the winter pole (90° N) shows only moderate enhancement over LTE, due to the small values of $\mathscr{R}$ at high latitudes (see Fig. 3) which result from the cold winter stratopause. In addition, below ~85 km, there is little atomic oxygen in polar night so that chemical pumping is virtually non-existent and therefore has almost no effect on the source function for this transition.

4. SUMMARY

By exploiting the physics of radiative transfer in upper mesospheric and lower thermospheric ozone, we have developed an algorithm to calculate accurately and efficiently the rate of radiative absorption by the v_3 fundamental band of ozone. This new algorithm is over four orders of magnitude faster than very detailed approaches used to calculate the radiative absorption rate. Source functions calculated using the radiative absorption rates from the new algorithm are essentially identical to those calculated using the rates from more time-consuming approaches. This new technique is readily applicable to studies of non-LTE processes in ozone and to radiance inversion algorithms used to determine the ozone concentration from i.r. emission measurements. Any error in the source functions introduced by using the new approach to calculate the radiative absorption rate is much less than the error introduced in the source functions due to uncertainties in the chemical pumping and vibrational relaxation mechanism.

Acknowledgements—We would like to thank S. Solomon of the NOAA Aeronomy Laboratory for providing the profiles of kinetic temperature and ozone that we used in our studies. We would also like to thank R. Boughner of NASA Langley Research Center for several helpful discussions pertaining to the correct formulation of the expression for the radiative absorption rate.

REFERENCES

1. M. G. Mlynczak and S. R. Drayson, *J. Geophys. Res.* **95,** 16497 (1990).
2. S. Solomon, J. T. Kiehl, B. J. Kerridge, E. E. Remsberg, and J. M. Russell III, *J. Geophys. Res.* **91,** 9865 (1986).
3. W. T. Rawlins, *J. Geophys. Res.* **90,** 12883 (1985).
4. M. G. Mlynczak, submitted to *J. Geophys. Res.* (1991).
5. S. Chandrasekhar, *Radiative Transfer*, Dover, New York, NY (1960).
6. M. G. Mlynczak, Ph.D. Thesis, University of Michigan, Ann Arbor, MI (1989).
7. L. S. Rothman, R. R. Gamache, A. Goldman, L. R. Brown, R. A. Toth, H. M. Pickett, R. L. Poynter, J. M. Flaud, C. Camy-Peyret, A. Barbe, N. Husson, C. P. Rinsland, and M. A. H. Smith, *Appl. Opt.* **26,** 4058 (1987).
8. S. R. Drayson, *JQSRT* **16,** 611 (1976).
9. S. R. Drayson, *Appl. Opt.* **5,** 385 (1966).
10. R. W. Sanders, S. Solomon, G. H. Mount, M. W. Bates, and A. L. Schmeltekopf, *J. Geophys. Res.* **92,** 8339 (1987).
11. R. R. Garcia and S. Solomon, *J. Geophys. Res.* **88,** 1379 (1983).
12. M. G. Mlynczak and S. R. Drayson, *J. Geophys. Res.* **95,** 16513 (1990).